Available online at www.sciencedirect.com
ScienceDirect
Journal of Nuclear Materials 367–370 (2007) 42–47
journal of nuclear materials
www.elsevier.com/locate/jnucmat

Irradiation effects on precipitation and its impact on the mechanical properties of reduced-activation ferritic/martensitic steels

H. Tanigawa [a,*], H. Sakasegawa [a], N. Hashimoto [b], R.L. Klueh [b], M. Ando [a], M.A. Sokolov [b]

[a] *Japan Atomic Energy Agency, Tokai, Ibaraki 319-1195, Japan*
[b] *Oak Ridge National Laboratory, Oak Ridge, TN 37831, USA*

Abstract

It was previously reported that reduced-activation ferritic/martensitic steels (RAFs) showed a variety of changes in ductile–brittle transition temperature (DBTT) and yield stress after irradiation at 573 K up to 5 dpa. The precipitation behavior of the irradiated steels was examined and the presence of irradiation induced precipitation which works as if it was forced to reach the thermal equilibrium state at irradiation temperature 573 K. In this study, transmission electron microscopy was performed on extraction replica specimens to analyze the size distribution of precipitates. It turned out that the hardening level multiplied by the square root of the average block size showed a linear dependence on the extracted precipitate weight. This dependence suggests that the difference in irradiation hardening between RAFs was caused by different precipitation behavior on block, packet and prior austenitic grain boundaries during irradiation. The simple Hall–Petch law could be applicable for interpreting this dependence.

1. Introduction

Material development for fusion reactors is now shifting to the engineering stage, as the ITER site was finally accepted to be Cadarash, France and therefore a schedule to build test blanket modules (TBM) becomes a practical necessity. Reduced-activation ferritic/martensitic steels (RAF) are the most promising structural materials for fusion power plant reactors from available candidates [1], because of the wide commercial production experience and the large database on similar materials. F82H (Fe–8Cr–2W–VTa) is one of the RAFs developed by Japan Atomic Energy Agency, JAEA (former JAERI) and JFE steel Co. (former NKK Co.) [2]. F82H has been distributed world wide as a part of an IEA program, with a database that has been accumulate for over 13 years with the efforts of various scientists/countries, it is now ready to be used for TBM design and construction.

Although the effort has reached the engineering stage, it is still very important to have the scientific

* Corresponding author. Tel.: +81 29 282 6498; fax: +81 29 284 3589.
E-mail address: tanigawa.hiroyasu@jaea.go.jp (H. Tanigawa).

0022-3115/$ - see front matter © 2007 Elsevier B.V. All rights reserved.
doi:10.1016/j.jnucmat.2007.03.167

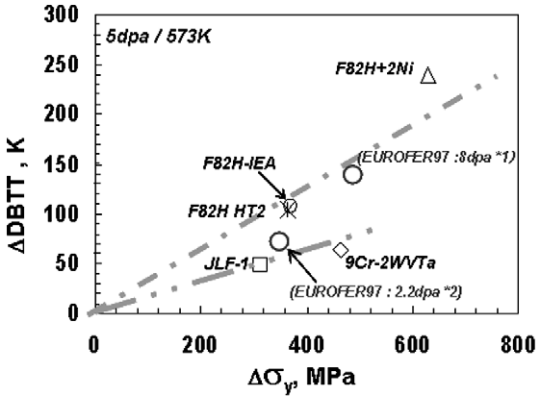

Fig. 1. Relation between DBTT shift and yield stress increase for various RAFs [3]. Data plots of EUROFER97 are based on the NRG final report by Rensman [4].

insight on what the database suggests about irradiation effects. It was previously reported that RAFs, such as F82H-IEA and its heat treatment variants, ORNL9Cr–2W–VTa (ORNL9Cr), JLF-1 as well as and 2%Ni-doped F82H, showed a variety of changes in ductile–brittle transition temperature (DBTT) and yield stress after irradiation at 573 K up to 5 dpa as shown in Fig. 1 [3,4]. It was especially difficult to understand why ORNL9Cr showed a smaller DBTT shift although it showed quite large hardening compared to other RAFs. These differences could not be interpreted simply as the result of Cr concentration difference, irradiation experimental error, or even as a simple effect of irradiation hardening caused by dislocation loop formation. To address these observations, the precipitation behavior of the irradiated RAFs was examined by weight analysis, X-ray diffraction analysis and chemical analysis on extraction residues [5,6]. In this study, the extraction replica analyses were performed to support the above research, and possible mechanisms were investigated based on these results.

2. Experimental

The material used was IEA-modified F82H (F82H-IEA), ORNL9Cr–2W–VTa (ORNL9Cr) and JLF-1 HFIR heat (JLF-1). Details of the chemical compositions are given elsewhere [3,5,6]. Block size analyses were performed on un-irradiated specimens using the orientation image mapping (OIM) system (Tex SEM Laboratories) for scanning electron microscopy (SEM) using an FE-SEM (Philips XL30), in order to analyze the grain orientation distribution. The OIM analysis was performed with a resolution of 200 nm and a 0.05 s exposure time per spot.

Irradiation was performed in the ORNL HFIR reactor to 5 dpa at 573 K in the removable beryllium (RB) position. Specimens selected for microstructure analyses were the 1/3 size Charpy specimens that fractured in a brittle mode (less than 1.0 J) on the lower shelf near the DBTT. Extraction replica samples were prepared from polished and etched 1/3 size Charpy specimens. TEM analyses were performed on replica samples.

3. Results

Fig. 2 shows the metallographic images and OIM results on the RAFs. The block size was analyzed based on these results by assuming that an adjacent grain with misorientation of less than 5° belongs to the same block. It turned out that the average block size for F82H, JLF-1 and ORNL9Cr are 49 μm, 29 μm, and 21 μm, respectively.

Fig. 3 shows typical TEM micrograph of extraction replicas which were obtained from each of the irradiated and un-irradiated RAFs. The size distribution and aspect ratio of precipitates were analyzed based on these micrographs, by ordering the precipitates in three categories: (1) precipitates on lath boundaries and in matrix, (2) precipitates on block and packet boundaries, and (3) precipitates on prior austenite grain (PAG) boundaries. It should be noted that the number density of precipitates on a replica is dependent on etching level, so the size distributions and shape distributions were

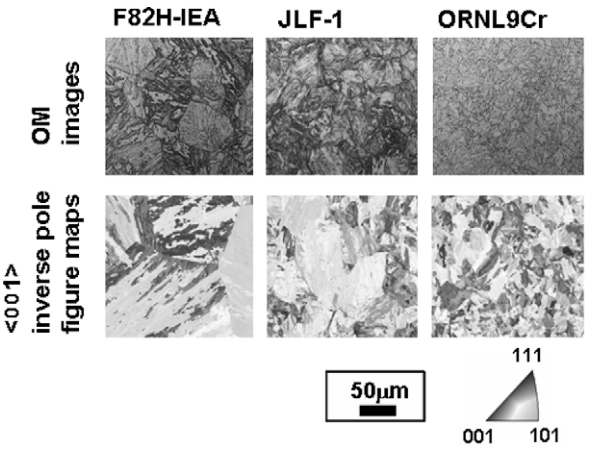

Fig. 2. Optical micrographs and orientation mapping of each of the RAFs.

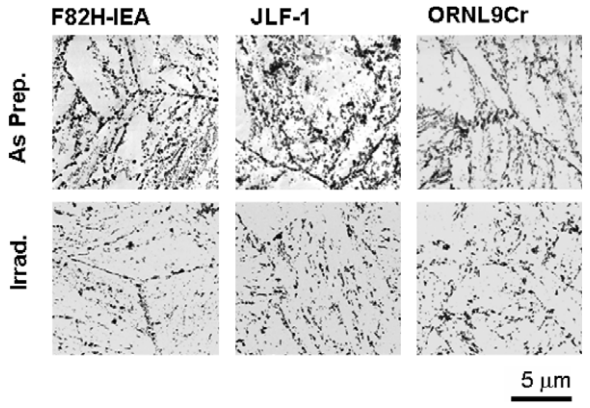

Fig. 3. TEM bright field images of extraction replicas obtained from each of the as-prepared/irradiated RAFs.

normalized to the total number of precipitate counted in the analyzed region. Since the precipitates exhibit various aspect ratios, the size of each precipitate was taken as the square root of the measured precipitate area. The analyzed results are shown in Fig. 4. The tendencies that could be determined from these results are as follows:

In the case of F82H: (1) small precipitates on lath boundaries or in the matrix are dominant in as-prepared sample, (2) precipitates on blocks, packets and PAG boundaries become dominant and elongated after irradiation and (3) the precipitates on lath boundaries or in the matrix become smaller and their density is reduced after irradiation.

In the case of JLF-1: (1) relatively larger precipitates are dominant on all boundaries in an as-prepared sample, (2) precipitates become smaller and more elongated with greater fraction, and the relative fraction increases on PAG boundaries after irradiation.

In the case of ORNL9Cr: (1) small precipitates on lath boundaries or in the matrix are dominant in an as-prepared sample, (2) precipitates become smaller and more elongated, and the relative fraction increases on block/packet boundaries.

4. Discussion

The defect number density and average size were measured based on the TEM images previously obtained [6,7] and the magnitude of hardening was calculated based on the Orowan model,

$$\Delta\sigma_y = T \cdot \alpha \cdot G \cdot b\sqrt{N \cdot d}, \tag{1}$$

where T is Taylor factor which gives $\Delta\sigma = T\Delta\tau$, is constant and $\alpha = 0.3$ for dislocation loop, G is the shear modulus (80 GPa), b is Burgers vector (0.268 nm) and N is the number density of loops and d is the average diameter of loops (Table 1). It appears that, the hardening level for JLF-1 shows good agreement, but it was underestimated for the other RAFs. This result suggests that there should be an other mechanism which could explain the extra hardening. Size distribution changes shown in Fig. 4 suggest that there is a general tendency for the precipitates on block, packet and PAG boundaries to become dominant after irradiation. Most of these precipitates are $M_{23}C_6$, because the XRD analyses on irradiated RAFs showed only the peaks corresponding to $M_{23}C_6$ [5]. Extrapolating from this tendency, it can be assumed that the Hall–Petch-like mechanism becomes effective after irradiation. Yield stress σ_y is described in the Hall–Petch model by the equation

$$\sigma_y = \sigma_i + k_y/\sqrt{D}, \tag{2}$$

where σ_i is Peierls stress, D is average diameter of grain, and k_y is the dislocation locking parameter which is described by the equation

$$k_y = \alpha'\sqrt{Gb\tau_c}, \tag{3}$$

where α' is a constant, and τ_c is the critical shear stress which is induced by dislocations accumulated at grain boundaries, and which activates dislocation sources in the adjacent grain. This τ_c is assumed to be altered by precipitate accumulation on block, packet and PAG boundaries, so it could be assumed that the increase in dislocation locking parameter Δk_y could correlate with the amount of precipitate, i.e.,

$$\Delta\sigma_y = \Delta k_y/\sqrt{D}. \tag{4}$$

Based on these assumptions, $\Delta\sigma_y$ of each RAF was multiplied by the square root of the block size, and plotted against the weight increase of precipitates, i.e., the increase of extraction residue's weight (Fig. 5). The strength change shows a linear dependence against the increase in extraction residue weight, and this indicates the possibility that a Hall–Petch-like mechanism is operating, though theoretical work is needed to explain how the dislocation blocking parameter change could be correlated with the increase in precipitate weight. It is worth noting that the reason that the Hall–Petch law does not work for the estimation of as-prepared

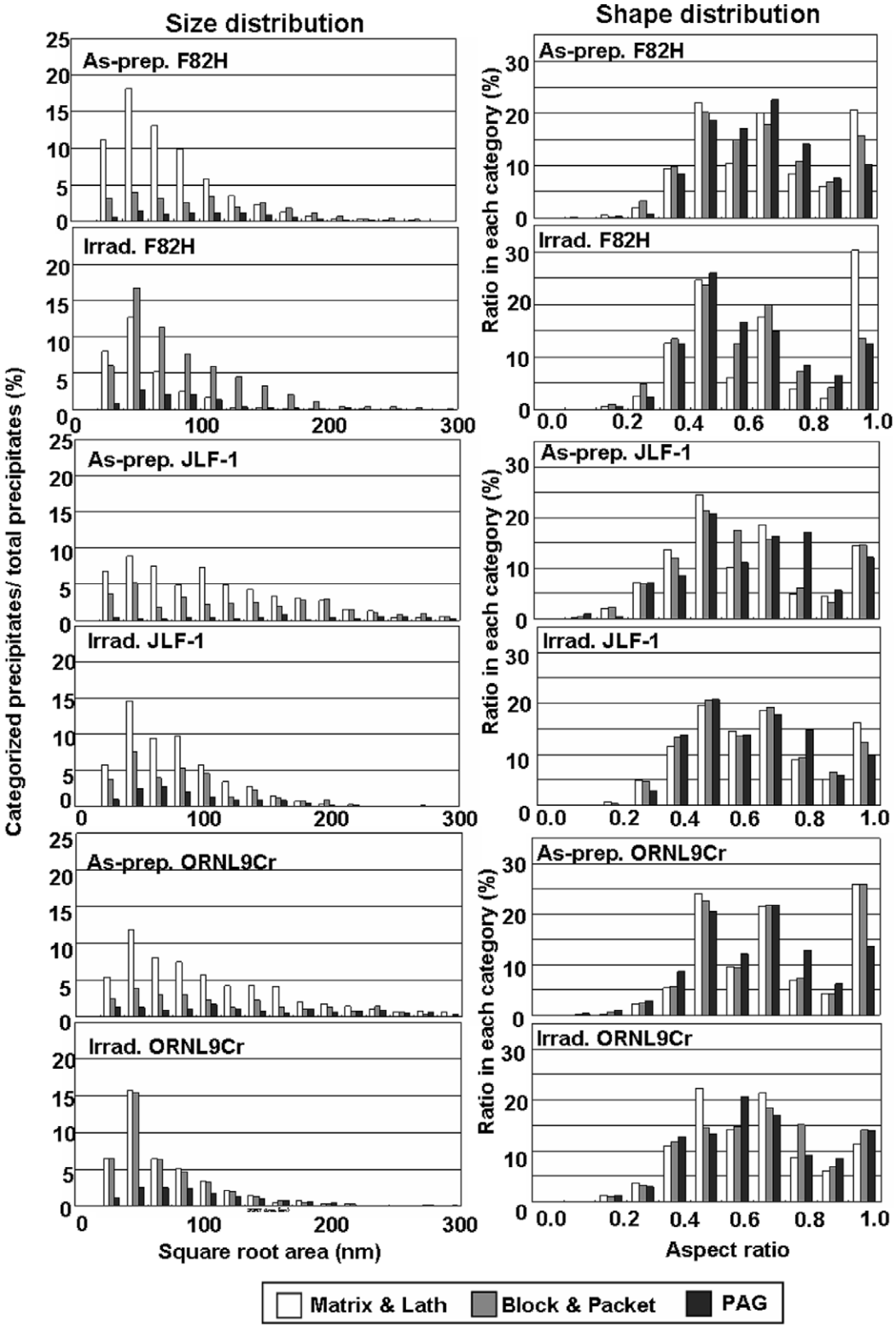

Fig. 4. Size distribution and shape distribution of precipitates.

Table 1
Dislocation loop number density and average size with estimated hardening

	Number density (10^{23}/m^3)	Average size (nm)	$\Delta\sigma_y$ (MPa)	
			Calculated	Measured
F82H_IEA	6.64	3.49	310	370
JLF-1	5.91	3.63	300	314
ORNL9Cr	7.59	4.19	363	463

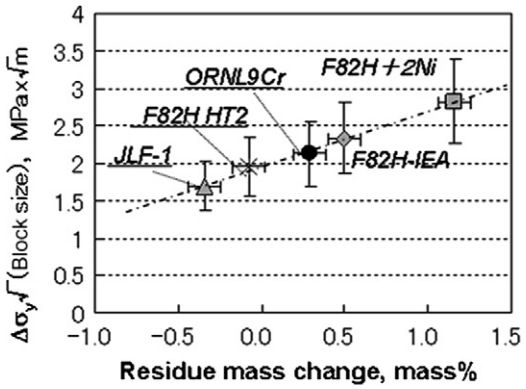

Fig. 5. Modified hardening dependence against the increase of extraction residue. $\Delta\sigma_y$ was multiplied by square root of average block size. Details on F82H + 2Ni (block size 29 μm) and F82H HT2 (block size 20 μm) are from Refs. [3,5–7].

RAFs could be because the precipitates are dominant on lath boundaries in as prepared RAFs, and the width of a lath is usually 200–300 nm and invariant between RAFs, so the effect of precipitates would be better treated with an Orowan model for as-prepared RAFs.

As previously discussed [5], the cleavage fracture stress σ_f must increase after irradiation, if it is assumed that the DBTT can be defined by the temperature that the flow stress becomes equal to the cleavage fracture stress. If it is assumed that the fracture initiates at precipitates on block/packet/PAG boundaries, working like a penny-shape crack with diameter equal to the average precipitate diameter, then σ_f could be expressed with the simple Griffith model, i.e.,

$$\sigma_f = \sqrt{\frac{\pi E \gamma_s}{2(1-\nu^2)C_0}}, \tag{5}$$

where E is elastic modulus, γ_s is surface energy, ν is Poisson ratio, and C_0 is the diameter of the penny-shape crack (i.e., average precipitate diameter). If it is assumed that there is no change in surface energy, then the ratio of fracture stress of irradiated specimen to that of as-prepared specimen could be described as,

$$\sigma_f^{\text{irrad.}}/\sigma_f^{\text{as-prep.}} = \sqrt{\frac{C_0}{C_0+\Delta C_0}}, \tag{6}$$

where ΔC_0 is the increase/decrease of initial crack diameter, i.e., the average precipitate size change. The estimated ratios are shown in Table 2. It turned out that the value shows good agreement in the case of JLF-1, but under estimate for F82H and ORNL9Cr. An other possibility that could increase the cleavage fracture stress is the amorphization of $M_{23}C_6$, which is reported in an other paper in this proceedings [8], which may increase the thresh hold energy for cracking precipitate, but this remains to be demonstrated.

5. Summary and conclusions

The precipitation behavior of three irradiated steels was examined in detail by analyzing extraction replica samples obtained from as-prepared and irradiated RAFs. The mechanism which controls hardening and DBTT shift after irradiation up to 5 dpa at 573 K is investigated in this study. The following is a summary of the important conclusions:

Table 2
Calculated fracture stress, compared with estimated fracture stress [5]

	F82H		JLF-1		ORNL9Cr	
	As-prepared	Irradiated	As-prepared	Irradiated	As-prepared	Irradiated
Average short axis length (nm)	75	55	103	59	91	48
Amount of large residue (wt%)	1.56	1.9	2.33	2.68	2.01	2.34
Calculated fracture stress ratio		*1.29*		*1.42*		*1.49*
Estimated fracture stress (GPa) [5]	1.68	2.7	1.86	2.66	2.09	3.38
Estimated fracture stress ratio [5]		*1.61*		*1.43*		*1.62*

C_0 and $C_0 + \Delta C_0$ are defined as the value proportional to the average short axis length multiplied by the amount of residue, in order to take the total precipitate mass change into account.

1. Size distribution of precipitates is changed after irradiation up to 5 dpa at 573 K; precipitates on block/packet and PAG boundaries tend to grow, and those on lath boundaries or in matrix decreased.
2. Hardening estimated from dislocation loop size distribution information was not sufficient to explain measured hardening levels for F82H and ORNL9Cr.
3. The Hall–Petch law may be applicable to explain the additional hardening for these RAFs.
4. The increase in cleavage fracture stress may be explained by the precipitation size change and amorphization.

Acknowledgement

This research was sponsored by the Japan Atomic Energy Agency; the Office of Fusion Energy Sciences, US Department of Energy under contract DE-ACO5-00OR22725 with UT-Battelle; and DOE/MEXT JUPITER-II Collaboration.

References

[1] K. Shiba, M. Suzuki, A. Hishinuma, J. Nucl. Mater. 233–237 (1996) 309.
[2] K. Shiba, A. Hishinuma, J. Nucl. Mater. 283–287 (2000) 474.
[3] H. Tanigawa, M.A. Sokolov, K. Shiba, R.L. Klueh, Fusion Sci. Tech. 44 (2003) 206.
[4] J. Rensman, NRG Final Report P68497C, NRG Petten, Netherlands, 2005.
[5] H. Tanigawa, N. Hashimoto, H. Sakasegawa, R.L. Klueh, M.A. Sokolov, K. Shiba, S. Jitsukawa, A. Kohyama, J. Nucl. Mater. 329–333 (2004) 283.
[6] H. Tanigawa, H. Sakasegawa, R.L. Klueh, Mater. Trans. 46 (2005) 469.
[7] N. Hashimoto, H. Tanigawa, M. Ando, T. Sawai, K. Shiba, R.L. Klueh, DOE/ER-0313/35, 2003, p. 41.
[8] H. Tanigawa, H. Sakasegawa, H. Ogiwara, H. Kishimoto, A. Kohyama, these Proceedings.